Computer-Aided Design ▮ (▮▮▮▮) ▮▮▮–▮▮▮

Contents lists available at ScienceDirect

Computer-Aided Design

journal homepage: www.elsevier.com/locate/cad

Efficient shape parameterization method for multidisciplinary global optimization and application to integrated ship hull shape optimization workflow☆

Ivo Marinić-Kragić*, Damir Vučina, Milan Ćurković

University of Split, Faculty of Electrical and Mechanical Engineering and Naval Architecture, Department of Numerical Modeling and Computer Application, R. Boskovica 32, 21000 Split, Croatia

ARTICLE INFO

Article history:
Received 2 March 2016
Accepted 5 August 2016

Keywords:
3D shape parameterization
B-spline
Multidisciplinary design optimization
Global optimization
Ship-hull optimization

ABSTRACT

Multidisciplinary global shape optimization requires a geometric parameterization method that keeps the shape generality while lowering the number of free variables. This paper presents a reduced parameter set parameterization method based on integral B-spline surface capable of both shape and topology variations and suitable for global multidisciplinary optimization. The objective of the paper is to illustrate the advantages of the proposed method in comparison to standard parameterization and to prove that the proposed method can be used in an integrated multidisciplinary workflow. Non-linear fitting is used to test the proposed parameterization performance before the actual optimization. The parameterization method can in this way be tested and pre-selected based on previously existing geometries. Fitting tests were conducted on three shapes with dissimilar geometrical features, and great improvement in shape generality while reducing the number of shape parameters was achieved. The best results are obtained for a small number (up to 50) of optimization variables, where a classical applying of parameterization method requires about two times as many optimization variables to obtain the same fitting capacity.

The proposed shape parameterization method was tested in a multidisciplinary ship hull optimization workflow to confirm that it can actually be used in multiobjective optimization problems. The workflow integrates shape parameterization with hydrodynamic, structural and geometry analysis tools. In comparison to classical local and global optimization methods, the evolutionary algorithm allows for fully autonomous design with an ability to generate a wide Pareto front without a need for an initial solution.

© 2016 Published by Elsevier Ltd.

1. Introduction

Multidisciplinary numerical shape optimization workflows for various technical objects have been developed in recent times. Efficiency of any shape optimization problem can be increased significantly by application of an appropriate shape parameterization method that keeps the shape generality while lowering the number of shape parameters. The optimization problem is furthermore difficult if global optimum is desired. Much research regarding global and multiobjective optimization in ship designs exists [1–9]. Various shape parameterization methods are applied, and it can be concluded that no superior shape parameterization exists [10].

Ship design problems normally include several objectives. For instance, the goals of the design process include single or multi speed resistance reduction, construction cost, reduced amplitude and acceleration of particular motions, particular quantities related to maintenance costs, etc. Most used objective in the ship design numerical workflows is hydrodynamic resistance minimization hence the application of trustworthy computational fluid dynamics (CFD) solvers is necessary and this is becoming a common practice in advanced ship design process [11,12]. Although computationally more efficient methods for resistance prediction exist, CFD is more flexible [12,13] as it can more accurately predict resistance of unusual shapes that can be created by the optimizer. Structural design optimization is another common optimization problem in ship design [14–16]. Typically improvement of a particular criterion causes deterioration of one or more others. It is intuitively recognized that such mutually conflicting criteria cannot all be met simultaneously; instead, compromises must be established. Two main approaches exist for solving multi-objective problems. The first is to combine all the objectives into a single one, usually based on economic merit [17]. The second approach is application of the Pareto optimality concept yielding multiple solutions where each one is better than all others in at least one objective.

Abbreviations: RPS, Reduced parameter set.

☆ This paper has been recommended for acceptance by Nickolas S. Sapidis.

* Corresponding author.
E-mail address: imarinic@fesb.hr (I. Marinić-Kragić).

http://dx.doi.org/10.1016/j.cad.2016.08.001
0010-4485/© 2016 Published by Elsevier Ltd.

Many papers have been published on ship simulation-based design [18,19], multi-objective ship optimization [2,4,20] as well as parameterization methods [3,5,21–23]. This paper aims at the development of a global multi-disciplinary optimization workflow without a need for initial solution. First, a sort of reverse engineering procedure for testing the proposed parameterization is implemented using the non-linear fitting procedure. The proposed parameterization methods are compared to classical B-spline-based parameterization with respect to the number of shape variables and root mean square fitting error (RMSE), on three different hull shapes. It was shown that the proposed shape parameterization does not have one-to-one mapping property as in some cases multiple genotypes can represent the same phenotype (in this case the same hull shape). The problem was solved by application of niching methods in the objectives space, ensuring population diversity for phenotypes. After the proposed parameterization is geometrically tested, two multi-objective optimization cases were conducted. This approach generates multiple Pareto optimal solutions in single optimization run and no initial solution is required.

2. Modeling for multidisciplinary ship hull optimization

Many objectives are possible in global ship optimization problem and in this paper only two are taken into account, minimal single-speed resistance and minimal structural mass. In addition to the objectives, the required constraints include the capacity, deck surface area and static stability. All constraints are easily calculated from the geometry using simple mathematics and in-house codes so only CFD and structural modeling are described in more detail.

2.1. CFD

For enhanced global optimization of a ship on the base of its resistance, an accurate CFD model is needed to guide the optimizer towards the optimal solution. With the recent breakthrough in ship CFD technology, practical applications of CFD have become possible [12,13].

A three-dimensional RANS model was used and implemented by commercial CFD code ANSYS FLUENT [24]. The SST k–ω turbulence model was used to close the governing RANS equations. Although the flow fields appearing in practical marine hydrodynamics are unsteady in nature, t is reasonable to assume that the flow around the ship is steady-state flow [12,19]. The main concern regarding the CFD in this paper is the reduction of the computational time such that the proposed parameterization method can be adequately tested on realistic time-scales. The proposed global optimization method and corresponding parameterization are not in any way limited to CFD as any ship hydrodynamic estimation method (e.g. the panel method) can be used in the developed integrated workflow. Accordingly an accurate ship CFD model for all Froude number regimes is not sought in this paper, but it is important that the targeted speed range is well covered.

Selecting an appropriate computational domain is the first step for accurate reproduction of fluid-dynamic phenomena. The choice of computational domain was based on previous works with a priority of reducing the computational effort as much as possible since CFD simulation will be plugged into the optimization workflow where many simulations will be conducted. To test the numerical model, the 5415 hull which has been adopted by the International Towing Tank Conference (ITTC) as a recommended benchmark for CFD validation for resistance and propulsion [25,26] was used. It was demonstrated by other authors (e.g. [27]) that an accurate CFD model is possible for the targeted speed range. Nevertheless a validation of CFD model will be conducted to confirm that the same accuracy is achieved. Since DTMB 5415 towing tank tests are used, the domain width was chosen (at first)

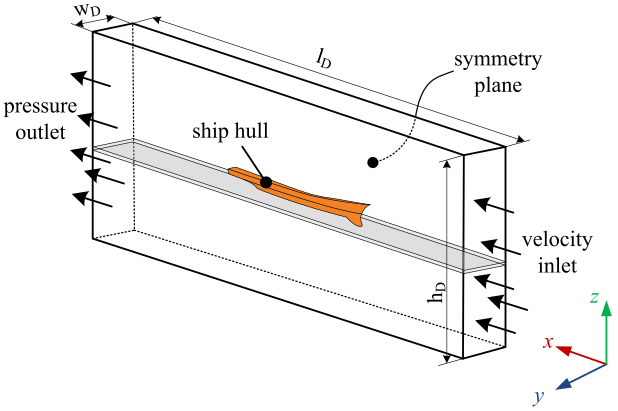

Fig. 1. Schematic of used computational domain: w_D-domain width, l_D-domain length, h_D-domain height.

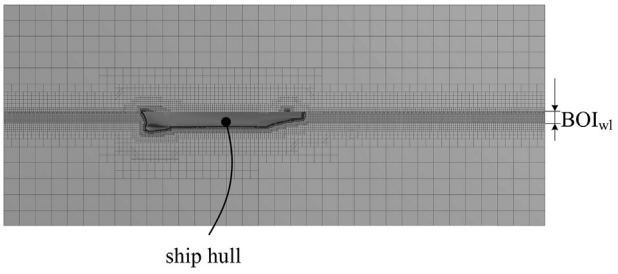

Fig. 2. Part of computational mesh with visible thickness of increased mesh density (T_{wl}) near the waterline.

to be equal to width of actual towing tank in experiment [28] while during the optimization run the half-width was set to 0.7L and depth was set to 2L. The length of domain was 2L upstream and 3L downstream (see Fig. 1).

The unstructured hexahedral grid was used as illustrated in Fig. 2. In order to get the best computational performance for each case of different hull shapes that appear during optimization, a special treatment would be required for each individual shape. That is not possible during optimization, hence a robust method that always generates a good quality mesh is required. The cut cell mesh generation method [29] is used, since it is robust, its generation does not require substantial computational time and has shown a better convergence rate in comparison to the tetrahedral mesh. This mesh is composed of cube-like elements that have a very low aspect ratio and skewness value A local zone of refinement is created near the free surface in the entire domain, to ensure a small enough z-grid spacing. A second refinement near the hull ensures small x- and y-spacing there to properly capture details of the free surface. A coarse mesh is used since precise results are not required in this paper and the goal is to test the proposed parameterizations for global multi-objective optimization of ship hulls. The Convergence criterion was set to 10^{-3}, this was enough to keep sufficient computational accuracy and maintain low time requirements. Typical number of mesh elements was about one million and each simulation takes about 1–2 h.

The comparison of the applied CFD model with experimental data [28] is illustrated in Fig. 3 where good accuracy of the applied numerical model is demonstrated.

2.2. Structural modeling

The design procedure turns out to be progressively complex as more subsystems are considered. Structural design optimization performed alone can require a large search and sometimes uses

Please cite this article in press as: Marinić-Kragić I, et al. Efficient shape parameterization method for multidisciplinary global optimization and application to integrated ship hull shape optimization workflow. Computer-Aided Design (2016), http://dx.doi.org/10.1016/j.cad.2016.08.001

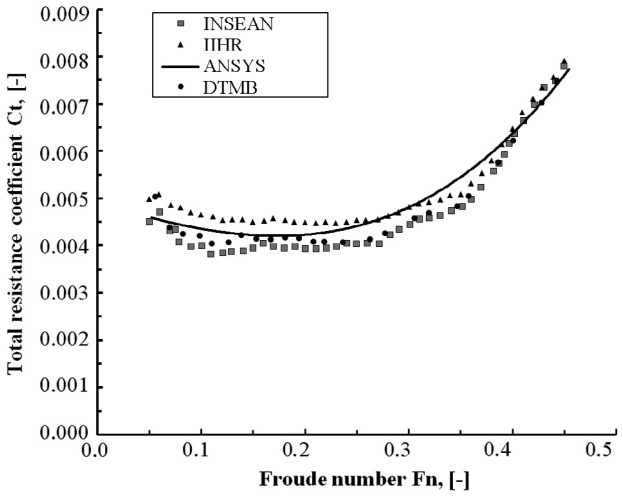

Fig. 3. Comparison between experimental data and CFD simulation.

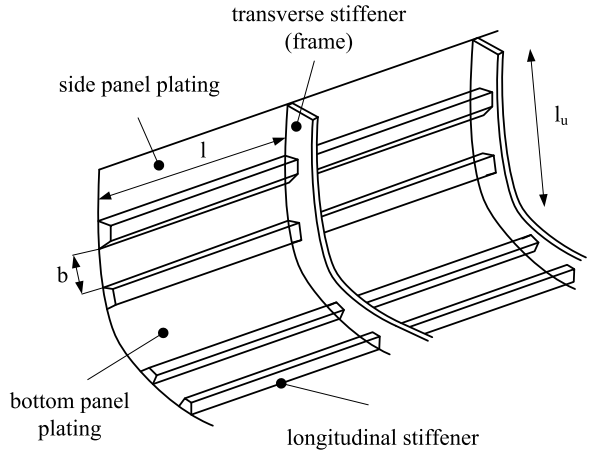

Fig. 4. Craft construction elements and important dimensions: l—panel large dimension, b—panel short dimension and l_u—unsupported stiffener length.

computationally expensive FEM tools. A first principles method can achieve a level of accuracy useful for early design without the requirement for expensive FEA techniques was used in this paper. Design rules have been developed on many years of experience and they are the main system for structural design of hulls used within the boatbuilding community. The hull was assumed to be built from composite materials which are attractive due to the ability to be tailored to various shapes. Standard ISO 12 215 has been developed for composite monohull scantling determination for small craft under 24 m. There are many papers discussing the ship structure optimization [14–16].

The determination of structure dimensions when using ISO 12 215 is based on the watercraft features and the environment that it is normally expected to be working in. The vessel structure can be divided in panels for which the standard is used to calculate pressure value on the basis of the panel position of within the hull form. For each panel, the minimal thickness is calculated using the pressure, the distance separating the stiffeners (long – l and short – s dimension –Fig. 4) and the curvature of the individual panel. Eq. (1) for calculating the minimal thickness $t_{\min}$ is given merely for clarification purposes. The layout of the full ISO 12 215 standard is out of scope of this paper, but from this single equation and explanation below, it should be clear how the standard was applied within this paper.

$$t_{\min} = \max\left(b \cdot f_k \cdot \sqrt{\frac{P \cdot k_2}{1000 \cdot \sigma_d}}, b \cdot f_k \cdot \sqrt[3]{\frac{P \cdot k_3}{1000 \cdot k_1 \cdot E_f}}\right) \quad (1)$$

where b is the short dimension of the panel (Fig. 4). f_k is a factor that depends on the radius of curvature of the panel (which can be calculated from the B-spline surface) and then the f_k value is obtained from tables within the standard. P is the design pressure that depends on the overall hull geometry (e.g. length, width, displacement, etc.) and the location of the panel (bottom, side, deck). The factors k_i depend on the aspect ratio b/l Fig. 4, and their values are given in tables within the ISO 12 215. The material is defined by the design stress σ_d and flexural modulus of elasticity, E_f.

This shows how the thickness of the hull depends only on simple geometrical relations (and material properties which are constant) that can easily be obtained from a B-spline surface that describes the ship hull. Similar equations are used to determine the minimal allowed stiffener geometry dimensions. The stiffener geometry is determined in a similar matter as thickness, by using the thickness of the adjacent panel and the design pressure P at the respective panel as input. Some of the most important (with respect to total mass of the vessel) craft construction elements such as panel and stiffeners are illustrated in Fig. 4.

It has been shown that using ISO 12 215 for structure optimization of composite boat hulls gives reasonable results [14]. Many design variables besides the hull form can be used [30] including internal compartmentation, machinery specs and structure. Although variables related only to the vessel structure such as distances between the stiffeners (b and l, Fig. 4) could easily be added as additional variables in optimization, this paper uses the design rules only for scantling and mass determination. The naval vessel hull shape is the only variable and all of the variables related to the structural analysis are calculated from the B-spline surface that represents the vessel hull. Variables related exclusively to the structure are not used since the primary objective of the paper is to prove that an efficient parameterization method for global optimization can be developed. The initial construction design topology was prescribed, and afterwards an automatic scantling method was implemented.

For a design generated by the optimizer, the draft is not known in advance but can easily be calculated from the total mass of the boat which includes prescribed equipment and crew weight, cargo and structure. Since the draft has an influence on both the pressure loads for individual panels as defined by the rules, a change in draft has an influence on structural mass, which again changes the draft and so on. This is solved iteratively for an individual design and the resulting draft is used as an input to the CFD simulation.

3. Ship hull parameterization

Given the fact that fully generic 3D shape modeling, complex 3D CFD simulations, and multi-objective global optimization are combined, a heavy computational effort of the respective integrated numerical workflow can be expected. Consequently an efficient shape parameterization is crucial for the optimization of respective geometry especially if imposing initial shape is not desired. If the parameterization is selected such that ship hull geometry can be described with a small number of parameters, the number of necessary simulations can perhaps be reduced enough to open a possibility of practical realization of global optimization procedures.

3.1. Parameterization

Traditional design of hull form is based on many points necessary to draw the body plan, waterline plan and profile plan. Using many shape parameters in modeling the 3D geometry of

Please cite this article in press as: Marinić-Kragić I, et al. Efficient shape parameterization method for multidisciplinary global optimization and application to integrated ship hull shape optimization workflow. Computer-Aided Design (2016), http://dx.doi.org/10.1016/j.cad.2016.08.001

the boat hull provides for faithful and accurate both local and global shape representation but is not adequate for optimization. Complex 3D shape is commonly represented by CAD models that contain many geometric primitives along with their attributes in addition to the relationships linking those entities. While this approach is sufficient for computer aided design it is a rather bad choice in the case of shape optimization. The most common approach is to use B-spline surfaces defined as:

$$S(u, v) = \sum_{i0=0}^{n0} \sum_{i1=0}^{n1} N_{i0,d0}(u) \cdot N_{i1,d1}(v) \cdot \mathbf{Q}_{i0i1}, \quad u, v \in [0, 1] \tag{2}$$

where $(n0 + 1) \times (n1 + 1)$ are the numbers of the control points, $N_{i0,d0}(u)$ and $N_{i1,d1}(v)$ are the basic B-spline functions of degrees $d0, d1 \in \mathbb{N}$ defined recursively as

$$N_{i,0}(t) = \begin{cases} 1, & t_i \le t < t_{i+1} \\ 0, & \text{otherwise} \end{cases}, \quad 0 \le i \le n + d$$

$$N_{i,j}(t) = \frac{t - t_i}{t_{i+j} - t_i} N_{i,j-1}(t) + \frac{t_{i+j+1} - t}{t_{i+j+1} - t_{i+1}} N_{i+1,j-1}(t), \tag{3}$$

$$1 \le j \le d, \ 0 \le i \le n + d - j$$

where:

$$\mathbf{t} = \{t_0, t_1, \ldots, t_{n+d+1}\}. \tag{4}$$

Eqs. (2)–(4) define the B-spline. As the individual shape functions $N_{i,j}(t)$ are non-zero just for the $[t_i, t_{i+j+1})$ interval, while amounting to zero for $t < t_i$ and $t \ge t_{i+j+1}$, the property of local control is ensured. As a result, the surface is formed exclusively by a small number of adjacent control points, $\mathbf{Q}_{i0i1}$. In this paper clamped knot vectors are assumed so that surface passes coincidently through the end curves. The shape of the surface is controlled by modifying the control points and the knot vectors. The properties of local support, partition of unity and non-negativity add to the numerical stability of the subsequent optimization procedure. B-spline and NURBS surfaces are flexible enough and provide sufficient degrees of freedom to represent the necessary shape for ship hull representation.

Various methods of application of B-spline and NURBS surfaces exist. One application of spline surfaces is the so called parametric design which can greatly improve the hull form description with respect to number of optimization variables. In [21], parametric modeling based on NURBS surfaces and curves is combined with CFD to improve hydrodynamic performance. The paper [5] conducts surface modifications using a shifting method and radial basis function (RBF) interpolation. This method provides for both global and local modifications of hull form and offers a possibility of reduction of the number of design variables, but this type of methods are not appropriate for optimization in the case of global optimization without an initial solution. In [31], a morphing tool is used to generate new hulls by deforming the initial hull shape. In a similar manner, the authors of [4] used a free-form deformation technique with large number of variables, for the optimization of an initial design of a fast catamaran.

In this paper an efficient global parameterization without the need to impose an initial hull shape was developed. The starting point for the idea leading to the proposed parameterization method is the following. A method sometimes applied for fitting splines curves is to modify the u and v parameters that define the end-points of spline so that in Eq. (2) $u, v \in [0, 1]$ is changed to u, $v \in [a, b]$, where $a, b \in [0, 1]$. The method is illustrated in Fig. 5 where an original B-spline curve is illustrated together with the effect of modifying the parameters u and v consequently changing the spline end-points.

While in the earlier method, curve end-points are modified in parametric coordinates (u and v) a similar effect is obtained by

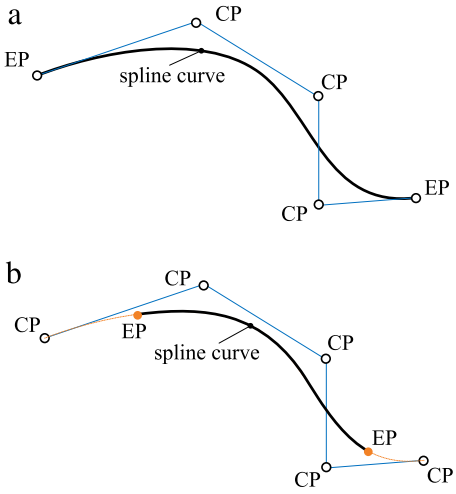

Fig. 5. End-points (EP) for spline curve with fixed control points (CP), with different parameter limit values: (a) original end-point parameter values (b) modified end-point parameter values.

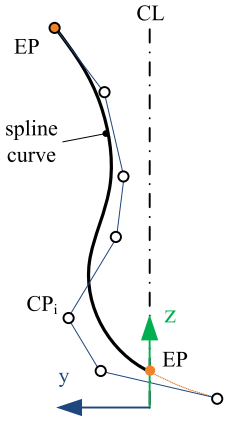

Fig. 6. End-points (EP) defined by the center line (CL) and $y > 0$ trimming.

trimming in physical coordinates. Now, the end-points are defined not only by the spline definition (2) but also by the spline location with respect to trimming line (or trimming plane for the case of surface). An example of spline trimmed by line is illustrated in Fig. 5, where the line designated as CL defines one of the end-points of spline curve. In this way, the B-spline curve or surface can still be defined by the modification of u and v parameters of the end-points but the end-points are fully defined by the trimming line or plane. In this paper, the center plane (similar to the center line in Fig. 6) is used for trimming such that the hull is defined only at $y \ge 0$. The same $y \ge 0$ trimming could be applied to any other surface representation used for description of ship hull such as NURBS, T-spline [32,33], RBF, etc. The limitation of this method is that only symmetric ship hull forms can be described, but since this is almost always assumed, it does not limit the application of the method considerably.

Application of this method does not by itself decrease the number of shape variables, although the freedom of shape is possibly increased. However, the method of constraining the spline to $y \ge 0$ allows for a big reduction of the multitude of shape variables as now the number of degrees of freedom for individual control point can be reduced to only one degree of freedom in y direction, as illustrated in Fig. 7. That is, x and z coordinates of each control point are set to the respective constant value. This way, each Fig. 7 can be represented by an isoparametric curve of B-spline surface, the curve also lies on $x = \text{const}$ plane. This method was named reduced parameter set (RPS) parameterization

Please cite this article in press as: Marinić-Kragić I, et al. Efficient shape parameterization method for multidisciplinary global optimization and application to integrated ship hull shape optimization workflow. Computer-Aided Design (2016), http://dx.doi.org/10.1016/j.cad.2016.08.001

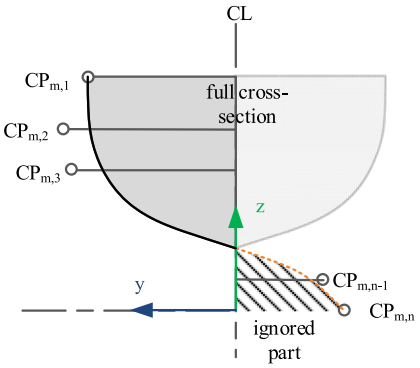

Fig. 7. Ship hull cross-section defined using reduced parameter set B-spline curve.

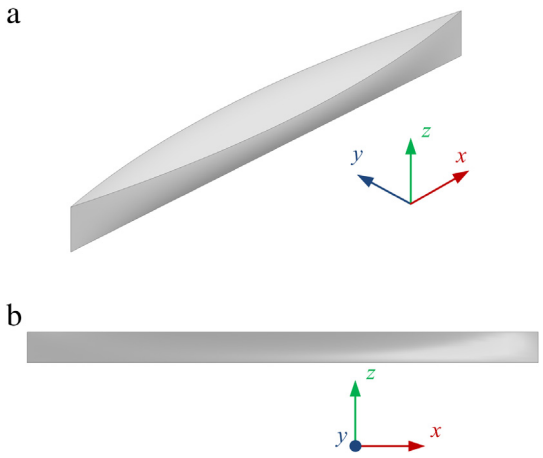

Fig. 8. Wigley hull: (a) isometric view and (b) view in y-axis direction.

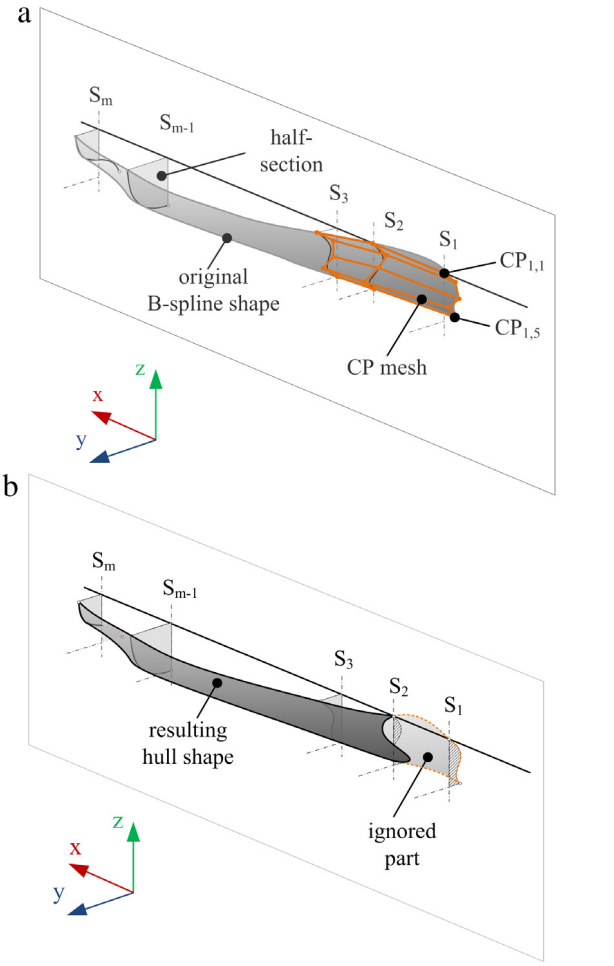

Fig. 9. Ship hull surface shape representation using B-spline surface defined with multiple sections (S_i) using reduced parameter set parameterization: (a) original B-spline surface and (b) resulting hull shape.

method. If the one variable per control point approach would be applied without the $y \geq 0$ trimming, the shape in side-view (y-direction) would always be a simple rectangular shape. Thus the RPS allows a possibility of significant shape generality increase while reducing the number of shape variables, and quantitative results will be given later in Section 5.1.

The shape variables are now the y coordinates of the control points $CP_{m,n}$ as illustrated in Fig. 7 for a single section and in Fig. 9(a), for the entire 3D hull shape where just two control points are designated ($CP_{1,1}$ and $CP_{1,5}$) and a part of control point mesh is illustrated for Sections 1–3. The RPS parameterization provides not only for shape representation but also for variations in shape topology. For example, as illustrated in Fig. 9(b), the bulb shape can easily be described with the same surface as the rest of ship. The trimming is not only applied for ships with bulbous bow but for essentially every shape except the ones that have rectangular shape (Fig. 8(b)) when viewing in y-axis direction such as the Wigley hull, Fig. 8.

With standard B-spline surface description, the bulb is usually described by an additional surface, whereby the continuity at the interface between the patches has to be imposed. Even more exotic topologies can appear during the optimization such as two hulls detached from each other. Since this paper deals with optimization of single ship hull, these occurrences are classified as unfeasible during the optimization run.

There exist some more realistic cases, for example a combination of a hull with accompanying objects (appendages) whose geometry is to be kept fixed. When using standard B-spline parameterization for the hull, the geometry of the appendages is usually modeled as separate entities by using CAD elements or again by using B-spline or NURBS. These separate geometric entities are then included as part of the overall geometry usually by using solid modeling. During optimization, these appendages would probably not be the object of optimization and would remain unchanged. The same can be accomplished by using RPS parameterization. Another optimization case would occur when most of the ship geometry is 'frozen' and only the bulb geometry must be optimized. The RPS parameterization can also be used here to describe the whole hull and just the control points that influence the shape of the bulb would be used in optimization. Since large computational effort of the CFD limits the number of variables to small multitude, it is not easy to obtain an optimal solution in a single optimization run. In those cases, the RPS parameterization could be used for initial global optimization with a small number of optimization variables (and control points). The solutions of the initial global optimization could then be used as initial geometries for optimization with larger numbers of control points. Local optimization could now be conducted using gradient methods for faster convergence despite the larger number of variables. Also additional degrees of freedom for the control points could be allowed for final fine tuning of the optimization procedure. These special cases will not be conducted in this paper, they were merely mentioned to point out that the RPS can be used for realistic cases with larger numbers of variables.

An unfavorable property of the proposed RPS parameterization is the non-uniqueness of mapping from the design variables space to the shape space Fig. 10. From the optimization point of view, non-uniqueness of mapping can cause problems such as poor convergence. One method of eliminating the possibility of multiple solutions that have different values of shape variables but the same

Please cite this article in press as: Marinić-Kragić I, et al. Efficient shape parameterization method for multidisciplinary global optimization and application to integrated ship hull shape optimization workflow. Computer-Aided Design (2016), http://dx.doi.org/10.1016/j.cad.2016.08.001

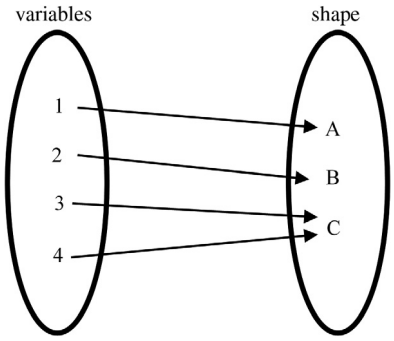

Fig. 10. Non-uniqueness of mapping shape variables to shape geometry.

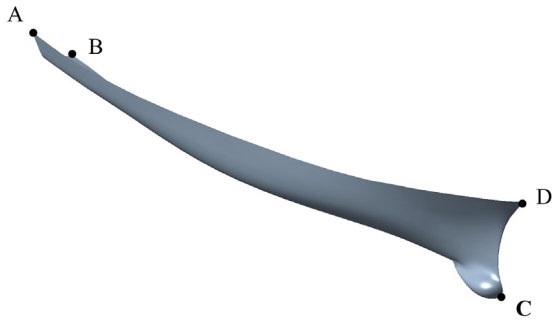

Fig. 11. DTMB half of ship hull.

geometry is by developing a niching operator as described in more detail in Section 4.

The basic RPS method—using one degree of freedom per control point does have some shortcomings and limitations. As an example, a hull shape that has a negative normal in y-axis direction could not be represented. This is not a serious limitation since such kinds of hull shapes are not common. Furthermore, the basic RPS method could be used at first to find a near global optimal solution using small number of optimization variables and genetic algorithms. The same spline surface could subsequently be used for local optimization by giving full 3D degrees of freedom for the control points and keeping the $y \geq 0$ trimming, thus eliminating the limitation on the surface negative y-axis normal. A modification of the basic RPS which can eliminate this limitation is also considered. The modified RPS method adds x and z components of individual B-spline rows (z-coordinates) and columns (x-coordinates) positions as two additional vector variables.

The geometrical test of the basic RPS, modified RPS and the full 3D parameterization methods will be conducted on three different hull shapes in Section 5.1. After the advantages of using RPS methods were confirmed, the feasibility of application for the global multi-objective optimization is still unknown since the RPS method possesses mentioned unfavorable properties. So the final two tests were the application of the basic RPS method on the local and global multi-objective ship optimization.

3.2. Evaluation of parameterization by shape fitting

To confirm that the proposed parameterization is superior to classical B-spline parameterization, a number of shape fitting tests were conducted on several point clouds that represent different hull shapes. The advanced method of non-linear fitting procedure similar to one in [34,35] was used as it allows for B-spline control points crowding and aggregation at locations of certain geometric features thus enabling good shape fitting while keeping low numerical complexity and high stability. The advanced fitting method is crucial since the linear fitting method cannot replicate the mentioned control point aggregation that occurs in actual optimization. If the ship hull geometry is obtained by 3D scanning, this procedure can be regarded as a reverse engineering [36] procedure, recent application includes [37–39]. The first step of the non-linear fitting method is a projection of point cloud $\boldsymbol{P}$ to a rectangular domain and obtaining an initial solution by linear fitting a B-spline to the projected point cloud. After the linear fitting, a gradient method and genetic algorithm are used for improving the solution. As opposed to classical B-spline fitting, the parametric coordinates (u and v) of the (point cloud) individual points are additional fitting variables that allow the B-spline control points movement towards locations of certain geometric features such as the bulb or hard-chine. In that case the error function subjected to minimization is:

$$E(\mathbf{U},\mathbf{V},\mathbf{Q}) = \frac{1}{2}\sum_{j0=0}^{m0}\sum_{j1=0}^{m1}\left|\sum_{i0=0}^{n0}\sum_{i1=0}^{n1} N_{i0,d0}(u_{j0j1}) \cdot N_{i1,d1}(v_{j0j1}) \cdot \mathbf{Q}_{i0i1} - \mathbf{P}_{j0,j1}\right|^2 \tag{5}$$

where $\mathbf{P}$ is point cloud matrix representing the hull shape; $\mathbf{U}$ and $\mathbf{V}$ are matrices of parametric values:

$$\mathbf{U} = \begin{bmatrix} u_{00} & \cdots & u_{0m_1} \\ \cdots & \cdots & \cdots \\ u_{m_00} & \cdots & u_{m_0m_1} \end{bmatrix} \tag{6}$$

$$\mathbf{V} = \begin{bmatrix} v_{00} & \cdots & v_{0m_1} \\ \cdots & \cdots & \cdots \\ v_{m_00} & \cdots & v_{m_0m_1} \end{bmatrix}. \tag{7}$$

For the initial solution, the $\mathbf{U}$ and $\mathbf{V}$ values are fixed and only the control points coordinates are obtained. Before obtaining the initial solution, an ordered structured point cloud is required such that it can be written in matrix form. In the case of the RPS parameterization, an ordered distribution of $\mathbf{U}$ and $\mathbf{V}$ is obtained easily by projection in y-axis direction and ignoring the $y < 0$ part of the domain. To obtain the required ordered distribution for $\mathbf{U}$ and $\mathbf{V}$ in the case of the full 3D spline fitting, a projection of shape from physical space to parametric space is required. The most-simple method is to use parallel sections (or waterlines) which can individually be projected to the respective location in the parametric domain. However this is not appropriate for a complex hull shapes such as DTMB hull illustrated in Fig. 11.

Fig. 12 illustrates the importance of the projection to rectangular domain. The line j-j which is the straight line with constant height that can easily be projected to $u - v$ domain by projection in y-axis direction. Similarly, the line k-k also appears that it can easily be projected but in a general case, line k-k is a 3D curve. The line designated l-l is obviously a 3D curve and it cannot be projected to the parameter space in a simple matter as the line j-j. This makes projecting 3D surfaces to rectangular domain a necessary step. The simplest method of projection to rectangular domain is obtained by applying the spring analogy to the meshed point cloud as presented in the paper [40] but a variety of different methods exist. In this paper a procedure from [34] is implemented since it demonstrated the best results. Regardless of the applied projection method, the result is a shape with rectangular boundaries in the parametric space as illustrated in Fig. 12(b). The required regular point grid can subsequently be created in the parametric space. New (regular) point coordinates in physical space are obtained easily by linear interpolation—mapping from parametric domain (Fig. 12(b)) to physical domain (Fig. 12(a)).

The method is briefly summarized here whereby the procedure will be illustrated on a half of the DTMB. The starting point of

Please cite this article in press as: Marinić-Kragić I, et al. Efficient shape parameterization method for multidisciplinary global optimization and application to integrated ship hull shape optimization workflow. Computer-Aided Design (2016), http://dx.doi.org/10.1016/j.cad.2016.08.001

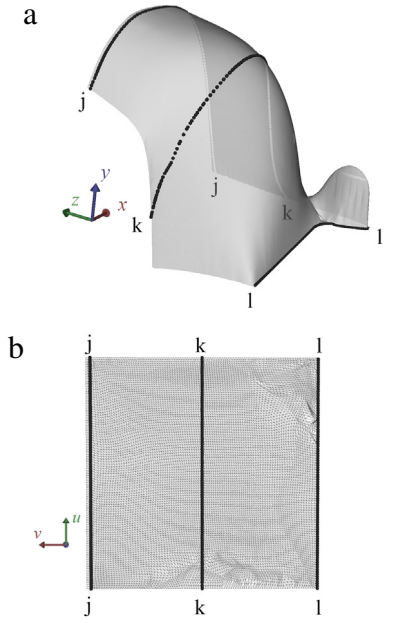

Fig. 12. Lines j-j, k-k and l-l illustrated in: (a) physical space (b) parametric space.

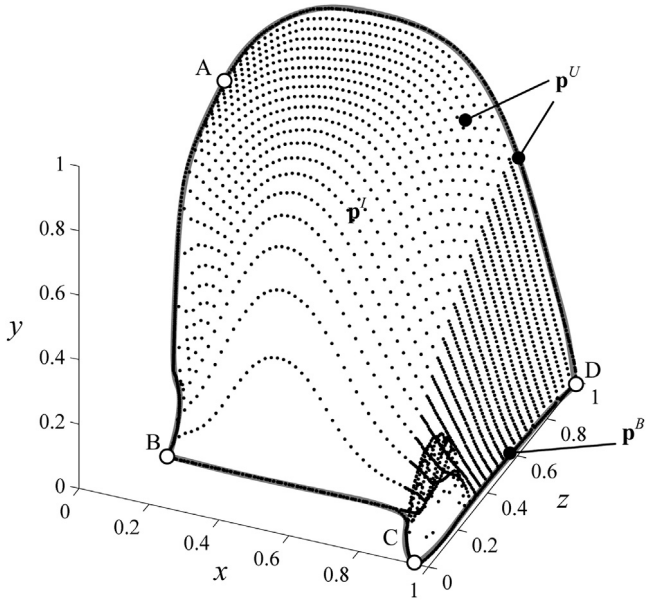

Fig. 13. Point cloud illustration: internal points, boundary points and corner points.

the projection method is a triangulated surface with an unordered point cloud $\mathbf{p}^U$ in physical coordinates as illustrated in Fig. 13. The unordered points $\mathbf{p}^U$ can be divided into two sets of points, the first set being the boundary points $\mathbf{p}^B$ and the second set of points the remaining internal points $\mathbf{p}^I$.

The first step is pre-projection of points ($\mathbf{p}_i'$) to parametric coordinates for which a simple y-axis projection can be used in case of half of ship hull. The next step is selecting four points on the geometry boundary $\mathbf{p}^B$, illustrated as small circles A, B, C and D Fig. 13. These points will be pre-set in the corners of the square $u - v$ parametric domain as illustrated in Fig. 14. Spacing of the rest of the boundary points when projected to the $u - v$ domain is linearly correlated to the physical distances between the points ($da''/da' = db''/db'$). The final step is moving of all of the pre-projected $\mathbf{p}_i''$ internal points to their final location in parametric domain. Procedure for individual point starts with arbitrary selection of angle αu. For the selected angle, $d_i'(\alpha)$ and $d_i'(\alpha + \pi)$ (physical distances between the point $\mathbf{p}_i$ and points xa' and xa') are calculated as illustrated in Fig. 14. The point $\mathbf{p}_i'$ is then translated to $\mathbf{p}_i''$ along the $xb'' - xa''$ line such that:

$$\frac{d_i''(\alpha)}{d_i'(\alpha)} = \frac{d_i''(\alpha + \pi)}{d_i'(\alpha + \pi)}, \tag{8}$$

where $d_i''(\alpha)$ is in-plane distance in the parametric domain. For the same point $\mathbf{p}_i$, the projection $\mathbf{p}_i''$ is calculated for multiple angles α and the resulting projection is obtained by averaging.

After projection of unstructured points $\mathbf{p}^U$ into the square parametric domain, the required matrix (for $\mathbf{U}$ and $\mathbf{V}$) topology of point cloud is obtained by simple interpolation. The fitting procedure is continued according to (5).

This brief section only illustrated a few key steps of the fitting method. The aim of this paper is not the testing of the methods from [34,35] or the spring analogy method from [40]. The goal is the application of the non-linear fitting methods to evaluate the proposed reduced-set parameterization. The original contribution of this paper is focused in using the non-linear fitting procedures for the purpose of evaluating suitability of various parameterization method for optimization. The comparison between the parameterization methods will be based on the root mean square error (RMSE) of the real distance from the point cloud to the spline surface:

$$RSME = \sqrt{\frac{1}{N} * \sum \left(\boldsymbol{X}_{Point\ cloud} - \boldsymbol{X}_{Spline}\right)^2} \tag{9}$$

where $\boldsymbol{X}_{Point\ cloud}$ is a point on the point cloud and $\boldsymbol{X}_{Spline}$ is corresponding closest point on the B-spline surface and N is number of used points. Point cloud points are taken by interpolation from the equidistant 100 × 100 grid from the projected $u - v$ domain as illustrated in Fig. 14 for both parameterization methods, such that the results can be compared. The closest point on the B-spline surface is found by the robust pattern search algorithm [41].

4. Optimization

In general, ship design problems are nonlinear and also non-convex, therefore excluding the possibility of using local optimization algorithms. The more suitable solution approach must adopt a global optimization scheme, since a local optimization algorithm cannot jump across the gaps created by the nonlinearities (constraints and objective function) to reach more favorable feasible regions of the design space. In addition, local optimizer can easily get stuck in suboptimal solutions near the initial design. To conduct a multidisciplinary global shape optimization, an optimizer has to integrate various performance analysis and geometric modeling tools with shape parameterization methods in form of a numerical workflow. The workflow consists of an evolutionary optimizer, structural scantling calculator, geometric properties calculator and CFD simulation programs as illustrated in Fig. 15 where horizontal direction represents process flow while the vertical direction represents simultaneous data flow. The computational workflow encapsulates geometric modeling (computer-aided design, CAD), simulation software (computational fluid dynamics, CFD) and calculators (structural, geometric characteristics) coupled with evolutionary numerical optimization. The numerical coupling needs to include the process executions and their mutual synchronization as well as data flows between the individual applications. Each vessel simulation starts after the optimizer generates values for the control points coordinates $CP_{m,n}$ (Figs. 7 and 9(a)). In the optimization case only the basic RPS method was used, thus the input parameters are the y coordinates for $CP_{m,n}$ control points. The

Please cite this article in press as: Marinić-Kragić I, et al. Efficient shape parameterization method for multidisciplinary global optimization and application to integrated ship hull shape optimization workflow. Computer-Aided Design (2016), http://dx.doi.org/10.1016/j.cad.2016.08.001

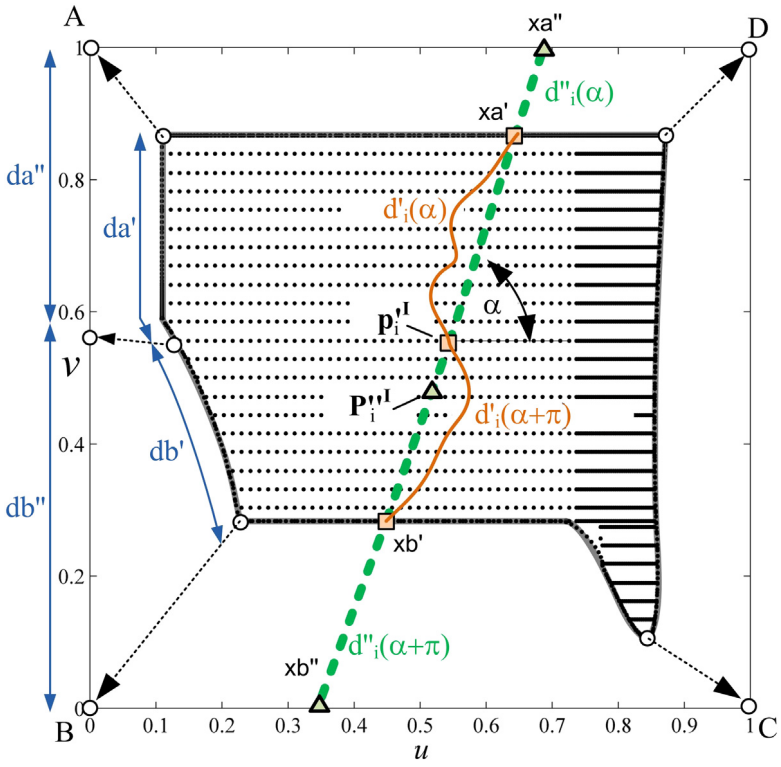

Fig. 14. Point cloud projected to rectangular parametric domain.

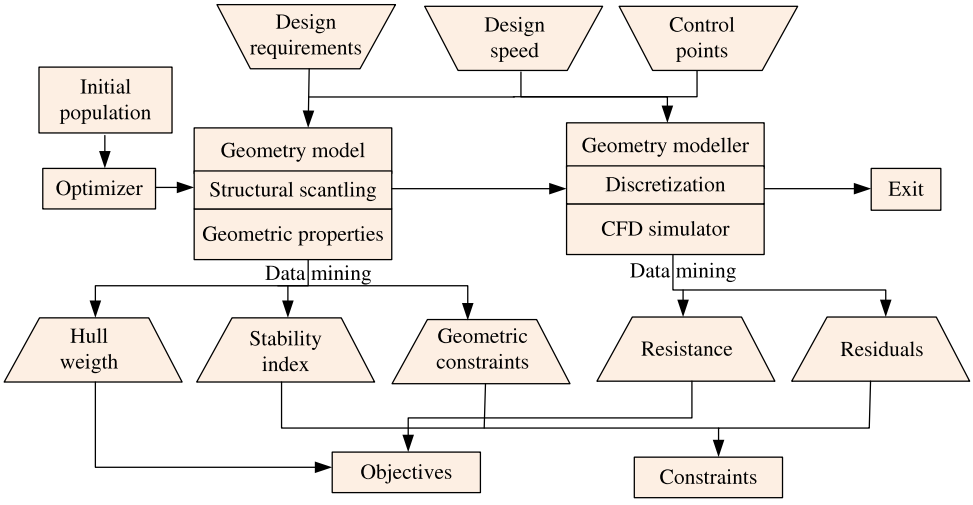

Fig. 15. Procedure of shape optimization and design synthesis controlled by an optimization algorithm.

values are at first taken from the initial population and later determined by the optimizer. The design speed and various design requirements such as capacity, deck area, and required stability are constant during a single optimization run. The structural analysis uses input values for control points to construct the B-spline surface and calculate the required geometrical characteristics to determine the dimensions and mass of the construction elements Fig. 4. Additional geometric properties such as displacement and deck surface area are calculated here. The design requirements together with the computed output values are now used to define the optimization constraints. For example the capacity constraint is defined such that the required capacity must be smaller than displacement minus total structural mass. After this, hydrodynamic simulation is conducted. The B-spline surface is communicated to the ANSYS Geometry Modeler [24] where trimming is applied, and based on trimmed surface solid modeling is used to define the volume that is used as input to mesh generation. The final step of a single vessel evaluation is completed after the CFD evaluates the hydrodynamic drag. Here, commercial software ANSYS Fluent [24] is used, although any kind of flow analysis can be plugged into the workflow. Both the structural calculator and CFD simulator produce large output files after they complete their assignments. Corresponding data mining (process of finding the required data in output files of simulation software) and coordination of the process flow was implemented using commercial software modeFRONTIER [42]. All of the calculations are executed on a single machine but in the case of practical applications the procedure should be parallelized [37].

The global optimization procedure is implemented using an evolutionary optimization algorithm, the used type of genetic algorithm was the MOGA-II [43] that can be used for single-speed optimization and eventually for robust (multiple speeds for a given

Please cite this article in press as: Marinić-Kragić I, et al. Efficient shape parameterization method for multidisciplinary global optimization and application to integrated ship hull shape optimization workflow. Computer-Aided Design (2016), http://dx.doi.org/10.1016/j.cad.2016.08.001

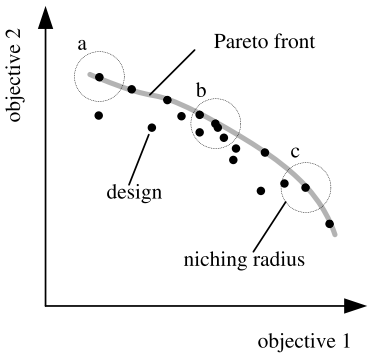

Fig. 16. Illustration of niching operator.

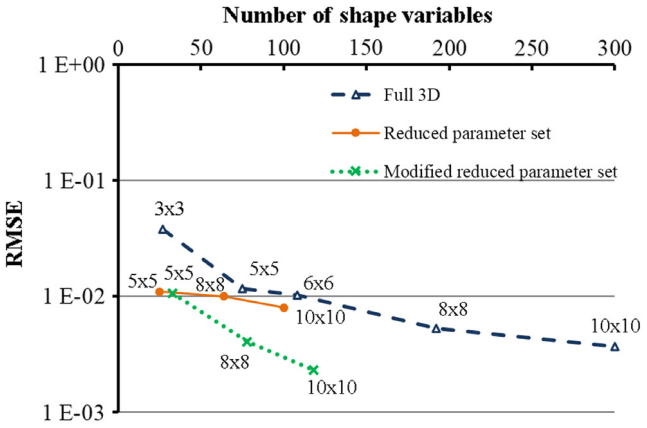

Fig. 17. Standard full 3D B-spline fitting compared to RPS parameterization with respect to the number of shape variables, comparison of fitting root mean square error of the fitting error for the DTMB hull shape.

speed distribution) optimization. Sobol initialization method [44] is used to initialize 500 designs as an initial population. The hull resistance (CFD) evaluation is the most computationally demanding task in the workflow (up to two hours of computational time) but during the optimization multiple simulations can be conducted simultaneously on a multiprocessor PC since genetic algorithm is used. The optimization procedure was stopped after 10,000 design evaluations (several months computational time on a standard PC) since the primary objective of the paper is to investigate the ability of optimization procedure to keep a wide Pareto front and prevent stagnation, and a near-global optimum is sufficient.

For the local optimization case, the Wigley hull is used as initial solution with initial length L = 20 m, width B = 2 m, height D = 1.5 m and draft T $\approx$ 1 m such that it geometrically coincides closely with dimensions used by other authors. In the case of Wigley hull optimization, a smaller initial population of 50 Wigley hulls (with very small random variations) is used. The optimization procedure was stopped if no significant improvement was observed for two subsequent generations. For both local and global optimization cases the design speed was $v = 4.4$ m/s corresponding to the Froude number $Fr = 0.314$ what is nearly the same as in the first case from [45] where $Fr = 0.316$. The hull geometry was described by a 5×5 control point mesh using the basic RPS parameterization method. The parameterization defines the hydrodynamically most important part of the hull $z = 0.0$ m–1.0 m, while the upper part is a simple extrusion of the $z = 1.0$ m cross section. The similar approach is used also by other authors. The geometrical constraints are minimal waterline moment of inertia of 1.4 m^4 and capacity (defined as displacement minus hull mass for the purpose of this paper) of 14,500.00 kg. Many other constraints and objective functions can and have been considered by various authors (for example [1,30]) but the selected constraints and objectives are sufficient for the parameterization test.

The one-to-one mapping problem can be solved by various methods. A simple approach would be to add a small penalty to the original objective function, where the penalty might be based on surface area or curvature of the original B-spline surface which includes the $y \leq 0$ part. The B-spline property of local support could also be used since it is easy to know based on the degree of spline how many successive control points have $y \leq 0$ coordinate, which control points do not influence the shape. Now, penalization can be added to all redundant shapes except for one or the penalty could be distributed across all of the shapes. This approach would be more computationally efficient since it does not require redundant computationally expensive CFD simulations. Here, an original, generic approach is applied by using a niching operator [46] related to the one in multi-objective optimization algorithms. The used approach is a bit less computationally efficient but it is robust and sufficient for the testing of the parameterization method. This approach adds penalty not only to the mutually identical shapes but to mutually very similar ones thus allowing for a smooth optimization procedure. The niching operators are implemented in MOGA algorithms to obtain a wider Pareto front. When they are not used, the Pareto front tends to concentrate on small areas that stalls the optimization process. The niching operator acts as a sort of penalty function added to the fitness function used to evaluate the performance of individual designs within the genetic algorithm. A type of niching operator, based on niching radius is illustrated in Fig. 16. The approach is based on counting the number of designs within some radius (in the objective space) for each individual design. Individual design fitness functions are then penalized by a value proportional to the number of designs counted in the niching radius around the design. For example, design "a" in Fig. 16 does not have any neighboring designs, so no penalty will be added. Meanwhile the design "c" has only one neighbor in the niching radius so a small penalty will be added while the design "b" has multiple neighbors such that larger penalty will be added to its fitness function. There are many types of niching operators, but each performs similar action of penalizing the designs in the design-dense area of the objective space. In this way, additional penalty functions that would be based on the inactive variables are not required. It was shown that the approach of using niching operators is sufficient since the optimizer has managed to maintain a wide Pareto front despite the inactive variables during the global optimization case presented in the next section.

5. Results and discussion

The results section is divided in two sections. The first section will evaluate whether the proposed parameterization can achieve the reduced space dimensionality without a loss in shape generality. After the proposed RPS has been confirmed to have the desired effect of reducing the number of optimization variables, the second part of the section presents the results of global and local multi-objective optimization test cases.

5.1. Comparison with standard parameterization

Two variations of the proposed parameterization are considered, the first is using only one variable per control point—the reduced parameter set (RPS) parameterization method. The second option is the modified RSP parameterization method by adding the control point grid column and row coordinates as additional variables. The fitting was tested using $n \times n$ B-spline grid sizes, where n was varied from 3 to 10 whereby larger values are not considered since they are not adequate for global optimization. The original

Please cite this article in press as: Marinić-Kragić I, et al. Efficient shape parameterization method for multidisciplinary global optimization and application to integrated ship hull shape optimization workflow. Computer-Aided Design (2016), http://dx.doi.org/10.1016/j.cad.2016.08.001

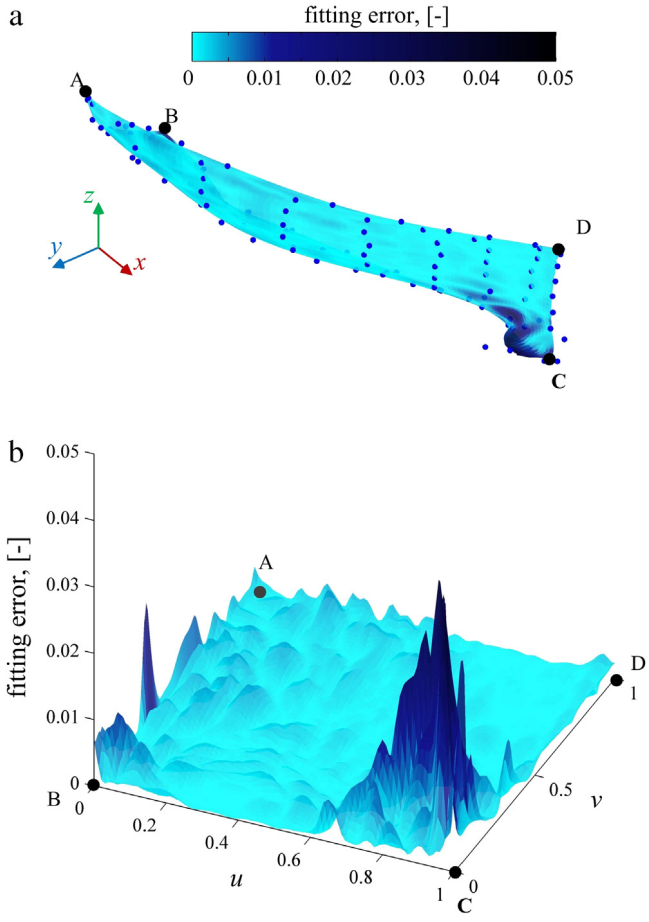

Fig. 18. Fitting error difference between the point cloud and B-spline surface for full 3D parameterization with 10 × 10 grid in: (a) physical coordinates (b) parametric coordinates.

hull point clouds are scaled to unit cube before the fitting procedure such that the results can be compared between individual fitting cases.

The first case, DTMB hull Fig. 11 is characterized by the complex shape of the "bulb-like" sonar dome suitable for parameterization using a separate parametric surface. The idea of the proposed parameterization was to increase the ability to handle these complex shapes. Fig. 17 shows the results of RMSE between the full 3D and the RPS parameterization methods for the DTMB hull with respect to number of shape variables and confirms that RPS methods yield better results. Both versions of the proposed parameterization show superior fitting performance in the investigated range of shape variables while the modified RPS version shows the most promising results.

The fitting error between the B-spline surface and point cloud for full 3D parameterization with 10 × 10 grid is illustrated in Fig. 18(a) where the distance is plotted on the hull surface. The fitting error was calculated from each point on the regular point cloud surface to the B-spline. A better visualization of the fitting error distribution can be obtained by plotting the fitting error in the parametric coordinates as Fig. 18(b) illustrates. As expected, most of the error is concentrated in the sonar dome area (near point C) of the hull amounting up to $3 * 10^{-2}$.

When comparing fitting errors for the same 10 × 10 grid size, the basic RPS method (Fig. 19(c)) yields larger fitting error values in all parts of the domain but the number of shape variables is three times smaller. The basic RPS method with the 10 × 10 grid has 100 shape variables that can be compared to the 6 × 6 full 3D parameterization (Fig. 19(a)) containing 108 shape variables. When comparing these two cases, the benefits of using the proposed parameterization are evident since the error is smaller in all parts of the hull geometry. The modified RPS method fitting error for the same 10 × 10 grid size is illustrated in Fig. 19(b), demonstrating exceptionally good results. In comparison to the basic RPS, the modified RPS method allows accumulation of the control point rows and columns in the areas of rapid geometry changes such as the sonar dome area. The RMSE even surpasses the full 3D parameterization for the same grid size while the number of variables is almost three times smaller.

The second test case is the relatively simple sailing yacht hull shape. As earlier, only half of the hull is used and corner points of the parametric domain are illustrated in Fig. 20. It is expected that this hull shape could be fitted fairly well with both parameterization methods since it contains no complex features.

In comparison to the DTMB shape fitting where even with a 10 × 10 control points grid a RMSE of 10^{-3} could not be achieved. Meanwhile, in this case of a relatively simple hull shape a RMSE of $0.9 * 10^{-3}$was obtained with full 3D parameterization. Meanwhile when using the modified RPS, a 15 × 15 control point grid was required to achieve RMSE under 10^{-3} amounts to a reduction in number of variables by 20% for the purpose of high accuracy fitting. When applying parameterization to the global optimization problem, 300 variables are still too much when complex CFD simulations are involved in shape optimization. Therefore, Fig. 21 illustrates the fitting error for grid sizes up to 10 × 10 and number of shape variables up to 100. For these low number of variables (<100), an even larger reduction in the number of variables for the same fitting error is obtainable with modified RPS. For example, a 5 × 5 fitting grid has almost the same fitting error for both the modified RPS and standard full 3D parameterization as illustrated in Fig. 21, which represents approximately a 50% reduction in the number of variables.

Meanwhile the basic RPS method did not achieve improvement over classical full 3d parameterization. Fig. 22 presents the comparison between all three methods for approximately the

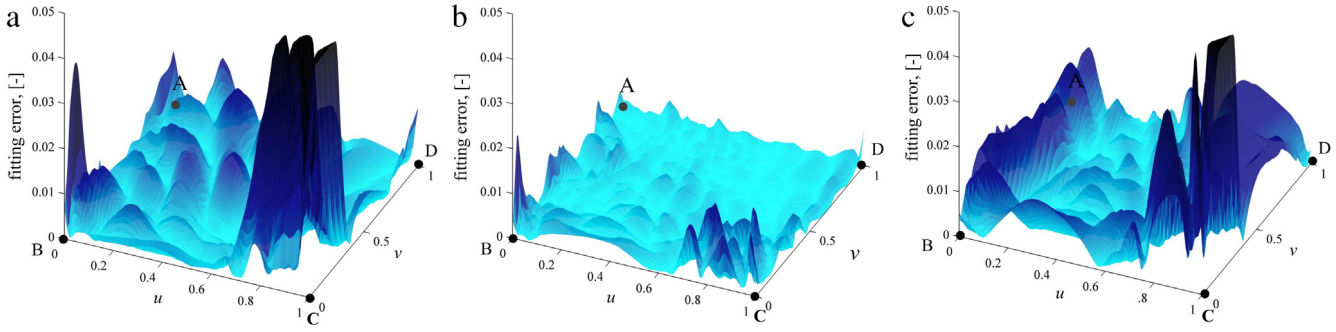

Fig. 19. Fitting error difference between the DTMB hull point cloud and B-spline surface for types: (a) full 3D parameterization with 6 × 6 grid; (b) modified RPS method with 10 × 10 grid; (c) RPS method with 10 × 10 grid.

Please cite this article in press as: Marinić-Kragić I, et al. Efficient shape parameterization method for multidisciplinary global optimization and application to integrated ship hull shape optimization workflow. Computer-Aided Design (2016), http://dx.doi.org/10.1016/j.cad.2016.08.001

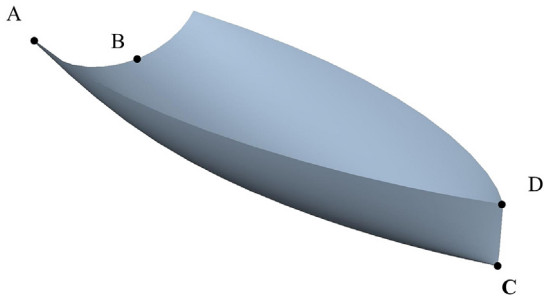

Fig. 20. Sailing yacht hull shape.

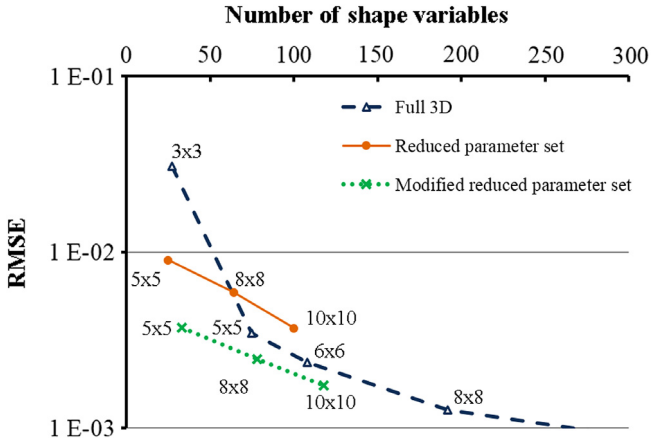

Fig. 21. Standard full 3d B-spline fitting compared to RPS parameterization with respect to the number of shape variables, comparison of fitting root mean square error of the fitting error for the sailing yacht hull shape.

same number (∼70) of variables. The modified RPS method shows the best results and has $\sim 10^{-3}$ fitting error on most of the shape except on the bottom area of the hull—near B-C line. In comparison, the full 3D method does not contain this error. The maximal error amounts to 0.015, 0.029 and 0.04 while standard deviation amounts to 0.0022, 0.0028 and 0.0039 for cases of full 3D, modified RPS and RPS methods respectively. This can be explained by the fact that the *y*-component of the normal on the hull in the symmetry plane tends to zero for the sailing yacht hull shape. In other cases this did not occur that is, lower RMSE is followed by lower maximum error and lower standard deviation. As pointed out earlier, the basic RPS is expected to yield poor results in these areas. Generally, a similar conclusion as in the DTMB case can be obtained; the modified RPS yields the best results. The basic RPS method was shown to be better than the full 3D parameterization only with a very low number of shape variables and its fitting performance deteriorates for more than 50 shape variables.

Since the first two test cases yield good results in favor of the proposed method, the last test case hull was selected such that the

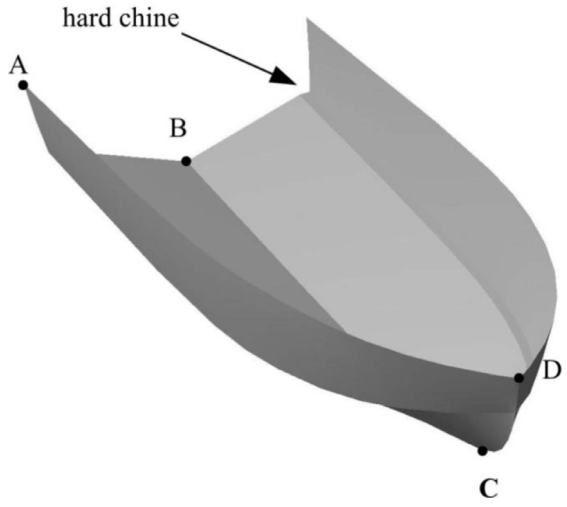

Fig. 23. Planing hull with hard chine.

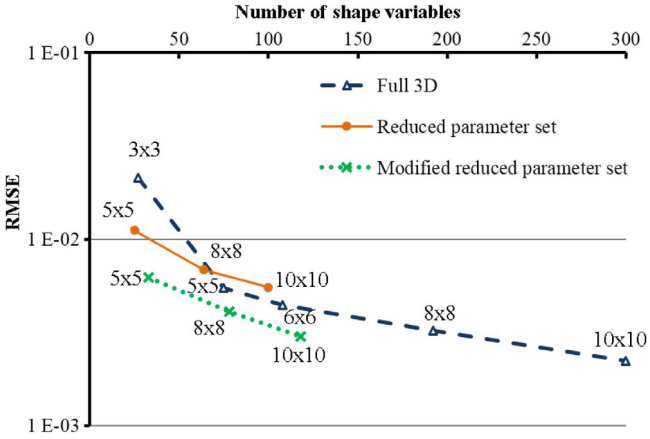

Fig. 24. Standard full 3d B-spline fitting compared to RPS parameterization with respect to the number of shape variables, comparison of fitting root mean square error of the fitting error for the planing hull with hard chine.

proposed method is initially expected to result in poor fitting. The initial expectation is based on the reduced ability to describe a hull shape with a normal pointing in the negative *y* direction (or equal to zero). The selected hull shape has a part of surface (hard chine, Fig. 23) with a surface normal *y*-component equal to zero.

As illustrated in Fig. 24, the basic RPS method shows reduced fitting performance for a >50 number of variables, while it surprisingly yields better results for the very low numbers of shape optimization variables. Furthermore, the modified RPS method shows better fitting results in all investigated cases in comparison to the full 3D parameterization.

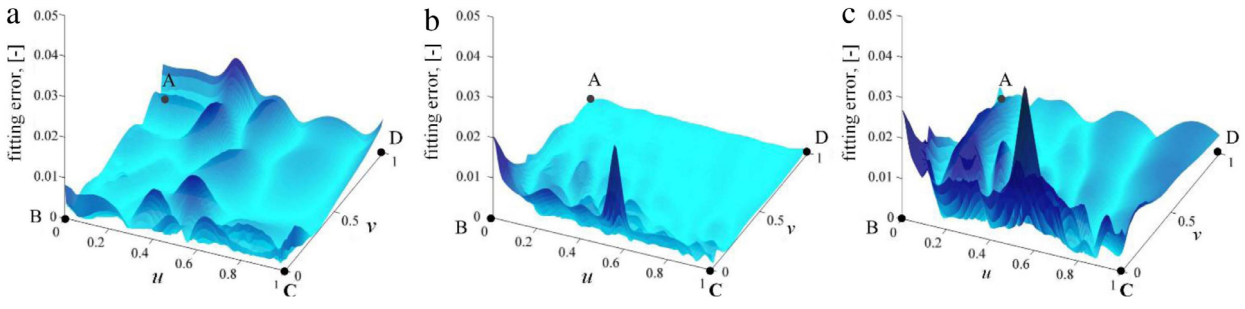

Fig. 22. Fitting error difference between the sailing yacht hull point cloud and B-spline surface parameterization for types: (a) full 3D parameterization with 5 × 5 B-spline grid; (b) modified RPS with 8 × 8 B-spline grid; (c) RPS with 8 × 8 B-spline grid.

Please cite this article in press as: Marinić-Kragić I, et al. Efficient shape parameterization method for multidisciplinary global optimization and application to integrated ship hull shape optimization workflow. Computer-Aided Design (2016), http://dx.doi.org/10.1016/j.cad.2016.08.001

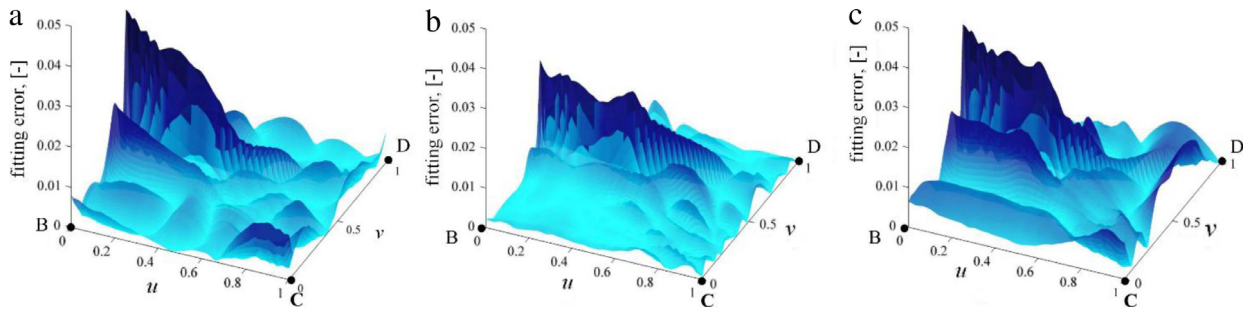

Fig. 25. Fitting error difference between the planning hull point cloud and B-spline surface parameterization for types (a) full 3D parameterization with 5 × 5 B-spline grid; (b) modified RPS with 8 × 8 B-spline grid; (c) RPS with 8 × 8 B-spline grid.

Fig. 25 illustrates the fitting error for approximately the same number of variables (∼70). Most of the error is now contained in the narrow area of the hard chine and in nearby areas (about halfway between points A and B) while the rest of the hull shapes results in relatively small fitting errors.

The results of all three cases show the benefits of the RPS methods in low and especially in the region of very low (<50) number of shape variables. This means that for the same number of variables, the proposed RPS method could obtain a solution closer to the global optimum. The larger shape generality is obtained with the same number of variables; correspondingly a reduction of the computational time could be obtained while keeping the same shape generality. Still the applicability of the method to the real case of optimization could become problematic because of the problems associated with the one-to-one mapping property some other unexpected difficulties could accrue.

5.2. Multi-objective optimization

In the previous section, the RPS parameterization has demonstrated better results in comparison to classical B-spline parameterization for the purpose of shape fitting. Shape fitting can be regarded as shape optimization if the shape (point cloud) to which the surface is fitted represents the actual optimal shape for some case. Three different shapes were used in the fitting examples, and each can be considered optimal for a maritime vessel in different operating conditions. The point clouds to which the surface is fitted are not actually optimal shapes but they have the most important geometric features that the optimal shape would have. For example a small vessel optimized for large Froude numbers would have a hard chine, Fig. 23. If a large maritime vessel is optimized for single speed, the resulting hull shape will have a bulbous bow. Although the example used here is the DTMB hull Fig. 11 with a sonar dome and not a bulbous bow, if a parameterization has a good capacity to represent the DTMB hull, it is expected that it will be good at representing the optimal hull shape that would appear during optimization of a large vessel optimized for a single speed. A small vessel that operates in a wide array of speeds would probably not have any specific geometrical features Fig. 20. Since the RPS parameterization illustrated better fitting (RMSE) in all three cases, it is expected that the optimization using the RPS parameterization will arrive closer to the optimal solution with the same number of optimization variables. Equivalently, a smaller number of optimization variables can be used and the resulting shape would be equally close to the optimal one. After the proposed RPS parameterization has demonstrated better results, the following optimization cases are conducted in order to confirm that the RPS parameterization can be used for "practical" optimization purposes. Since the one-to-one mapping problem could possibly prevent convergence, one of the main objectives of this section is to demonstrate that the proposed parameterization method can be used for actual optimization.

As for the smallest grid sizes the RPS method provided the best results earlier in comparison to full 3D parameterization method, and computational expensive CFD constrains number of evaluations, the 5 × 5 B-spline control points grid is selected. Only the basic variation of RPS parameterization is used to conduct the optimization cases. The results are presented for two cases of multi-objective optimization of a small vessel. The first case is the local optimization case with the Wigley hull as a starting solution. The second case uses the same parameterization as in the first case, but starts from randomly generated initial population. The individual feasible designs in the objective space after 20 generations for both optimization cases are illustrated in Fig. 26 where the number of points (optimization designs) is reduced for better clarity.

Fig. 27(a) illustrates the starting solution for the local optimization case half-sections. The middle half-section is the widest section on the right part of the figure and rest are equally spaced half-sections towards the ship bow. The stern-wise part of ship is illustrated in the similar manner but on the left side of the figure.

Fig. 27(b) illustrates a hull on the minimum resistance side of case 1. The hull has the same tendency as in [19] where the Wigley hull, when used as a initial geometry, has a tendency to reshape the bow into a shape similar to one generated here. While the Wigley hull hydrodynamic resistance amounts to 2.17 kN, the reduction to 1.95 kN is obtained by minimization of resistance. The simultaneous reduction of the hull mass (on the other side of the Pareto front) results in the hull shape illustrated in Fig. 27(c). The half-sections are a bit bulkier and an increase from 1.95 to 2.16 kN of resistance (see Fig. 28) is followed by a small reduction in hull mass from 1596 to 1579 kg.

The comparison of Pareto front sizes Fig. 26 of the two cases illustrates a huge advantage of using global optimization. Nevertheless local optimization starting from the Wigley hull yields good results as the Pareto front coincides with the global optimization case. Only a modest change in mass from one to the other side of the Pareto front was obtained in the former while the for the global optimization case it varies from 1312 to 1606 kg. The difference in the hydrodynamic resistance is considerable as it ranges from 3.54 to 1.77 kN. In [19], the optimized hulls reduction in hydrodynamic resistance with respect to the Wigley hull amounts 17.4% which is similar to the one obtained here amounting to 18.4%. The result can be different since the hydrodynamic simulation analysis methods were not the same. More detailed results for the selected designs are presented in Table 1 where hydrodynamic, geometric and structural characteristics.

The lowest-mass solution from global optimization results is illustrated in Fig. 29(a). For this design, the hull length is decreased to 13.6 m while still satisfying the constraints related to displacement and waterline moment of inertia. This is possible since the width has increased considerably and the design is also accompanied by an increase in hydrodynamic resistance to

Please cite this article in press as: Marinić-Kragić I, et al. Efficient shape parameterization method for multidisciplinary global optimization and application to integrated ship hull shape optimization workflow. Computer-Aided Design (2016), http://dx.doi.org/10.1016/j.cad.2016.08.001

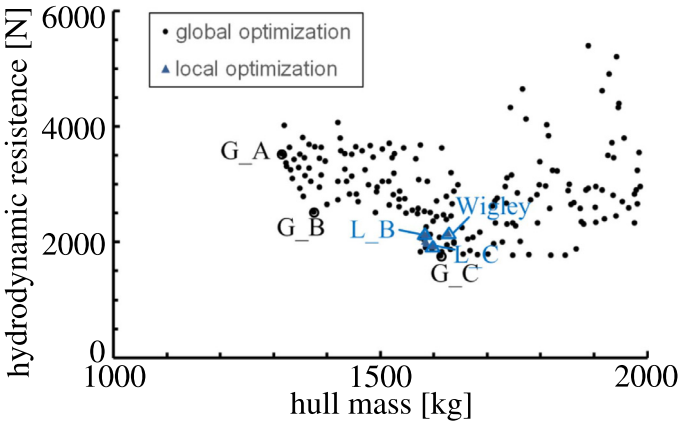

Fig. 26. Designs from both local and global optimization case plotted in optimization criteria space.

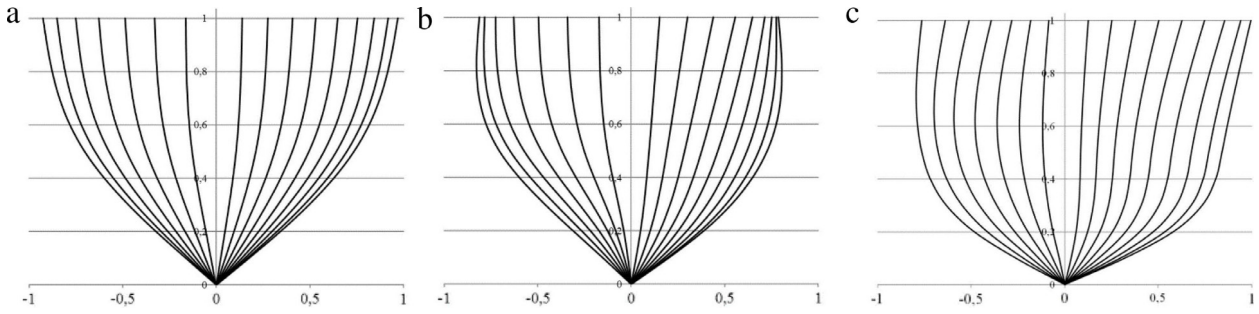

Fig. 27. Half-sections for designs: (a) The Wigley hull (b) L_B design (c) L_C design.

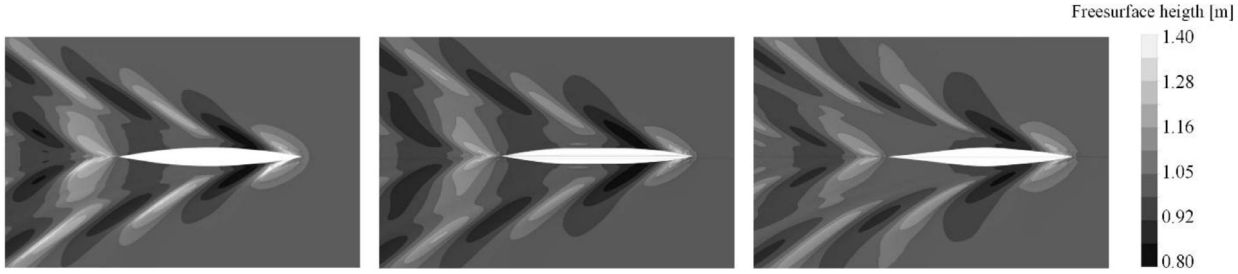

Fig. 28. Free-surface height for local optimization designs: (a) initial design—Wigley hull (b) L_B design (c) L_C design.

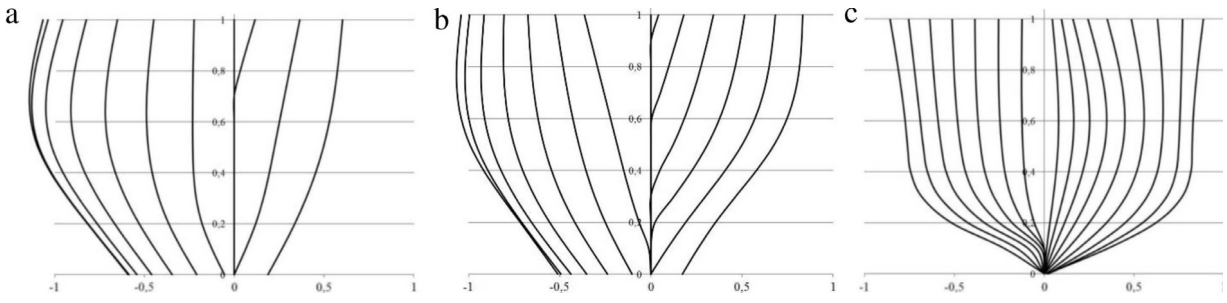

Fig. 29. Pareto individuals: (a) G_A design (b) G_B design (c) G_C design.

3.54 kN. The important feature to notice about this design is that about half of hull shape B-spline control points are located in the y negative area. The control points at the bow have practically no impact on the resulting hull shape but still the optimizer managed to find the solution in the integrated procedure with computationally expensive CFD simulation. Going along the Pareto front, the solutions of continuously increasing the length appear as illustrated in Fig. 29(b) with 16.0 m length, 1374 kg mass and 2.53 kN hydrodynamic resistance. The design Fig. 29(c) represents a design with minimal resistance of 1.77 kN and small hull mass amounting 1606 kg and is located in area close to the Pareto front of the first case. Further reduction of resistance (see Fig. 30) is negligible and followed with large hull mass requirements.

Finally note the increase of block coefficient (ratio of vessel displacement to a block of the same width, length and draft) in global optimization for cases G_A and G_B. This cases correspond to considerable decrease in hull structural mass and decrease in hull length. The increase of the block coefficient is possible because

Please cite this article in press as: Marinić-Kragić I, et al. Efficient shape parameterization method for multidisciplinary global optimization and application to integrated ship hull shape optimization workflow. Computer-Aided Design (2016), http://dx.doi.org/10.1016/j.cad.2016.08.001

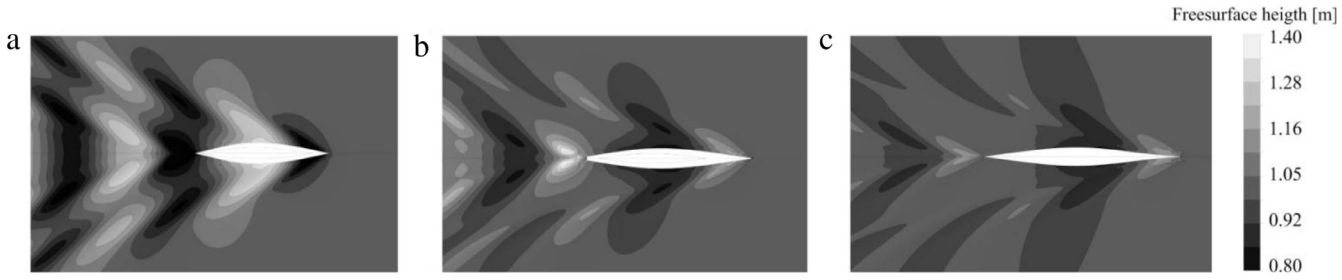

Fig. 30. Free-surface height for global optimization designs: (a) G_A design (b) G_B design (c) G_C design.

Table 1
Partial results of structural scantling calculation, hydrodynamic resistance and geometric characteristics for selected local (L) and global (G) optimization cases. A—cross sectional area, SM cross sectional modulus.

Design	Wigley hull	L_B	L_C	G_A	G_B	G_C
Hydrodynamic resistance (kN)	2.17	2.16	1.95	3.54	2.53	1.77
Hull mass (kg)	1625	1579	1596	1312	1374	1606
Length (m)	20.0	19.9	19.8	13.6	16.0	19.4
Beam (m)	2.0	1.64	1.94	2.14	2.11	1.92
Draft (m)	0.98	0.99	0.95	0.98	0.96	0.98
Displacement (m^3)	16.1	16.1	16.1	15.8	15.9	16.1
Waterline moment of inertia (m^4)	2.07	1.43	1.60	1.75	2.03	1.41
Bottom pressure (kN/m^2)	58.4	52.1	59.5	69.4	65.0	41.2
Bottom plate thickness (mm)	8.4	8.0	8.4	7.9	7.6	7.4
Longitudinal stiffener, A (cm^2)	16.2	16.0	16.2	13.5	15.2	14.0
Longitudinal stiffener, SM (cm^3)	58.4	56.2	58.1	44.6	51.9	45.6
Transversal frame, A (cm^2)	18.2	17.4	18.4	16.5	17.4	15.2
Transversal frame, SM (cm^3)	67.7	62.8	68.6	58.4	62.8	51.2

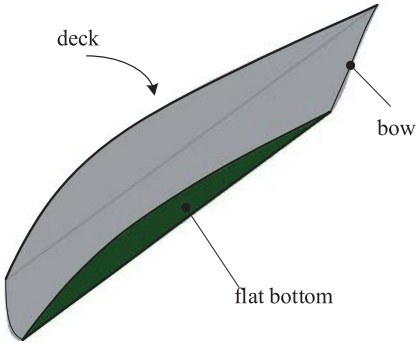

Fig. 31. 3D view of flat bottom for design G_A.

the hull now has a flat bottom as illustrated in Fig. 31 for the G_A design.

6. Conclusion

Two proposed reduced parameter set (RPS) shape parameterization methods have been compared to classical B-spline parameterization. It has been shown that the proposed shape parameterization methods are able to keep the shape generality while lowering the number of shape parameters on three mutually different test shapes. This means that for the same number of variables, the proposed RPS method could obtain a solution closer to the global optimum or likewise a reduction of the computational time could be obtained while keeping the same shape generality. Non-linear fitting method has shown an ability to be used as a performance prediction tool for shape parameterization before the actual optimization. Both proposed RPS methods have shown good results for DTMB shape containing a bulb-like sonar dome where a reduction of shape variables by a factor of three was obtained. Some difficulties have appeared with describing a hull shape with a normal pointing in the negative y direction, but the RPS methods have shown advantages in all cases. While the modified RPS method has kept the advantage over classical parameterization for other test cases and number of shape variables, the basic RPS method shown good results only for low number (<50) of shape parameters.

The developed multidisciplinary workflow integrating the proposed shape parameterization, hydrodynamic prediction tool and structural scantling rules proves that it is possible to have a numerical procedure that autonomously synthesizes the 3D shapes. Successful application of the basic RPS method has showed that the parameterization is suitable for global shape optimization. This novel shape parameterization approach has enabled a global optimization procedure that can start without an initial solution and result in wide Pareto front. Similar reduction of hydrodynamic resistance has been obtained as with other authors but the approach used in this paper allows for various compromises between the structural mass and hydrodynamic performance. Only one local and one global optimization case was presented in this paper although variations of global optimization case could be (and were) undertaken. The presented optimization case has illustrated the primary goal of this paper, to show applicability of the proposed parameterization method to multidisciplinary global optimization without an initial solution.

3D CFD was used for hydrodynamic resistance prediction, and an accurate prediction of the resistance for DTMB and Wigley hull were achieved. Nevertheless the results of the resistance simulation and used structural scantling method do not necessarily have to be reliable for a wide array of generic shapes that the optimizer is able to generate. This does not have impact on the good results that the presented parameterization method has illustrated regarding its ability of better fitting to various shapes and proven applicability to a global optimization. Using ISO 12 215 standard for structure scantling or 3D CFD for resistance estimation is not of any particular importance. The same parameterization method could be applied with any combination of structural scantling and hydrodynamic resistance evaluation tools and even other objective functions could be added. Furthermore the proposed parameterization procedure could be suitable for

Please cite this article in press as: Marinić-Kragić I, et al. Efficient shape parameterization method for multidisciplinary global optimization and application to integrated ship hull shape optimization workflow. Computer-Aided Design (2016), http://dx.doi.org/10.1016/j.cad.2016.08.001

applications beyond that of ship optimization. The procedure is suitable not only for generic optimization of planar symmetric shapes but axisymmetric shapes or it could be used in cases where part of the geometry is constrained while a part is subjected to optimization.

Since the full 3D CFD results in an optimization procedure with intensive computational resource is demanding, further approaches to reducing the computational time are required. A multi fidelity approach regarding resistance prediction methods implementing surrogate models will be investigated in future work. To additionally improve convergence, other optimization algorithms will be tested along with MOGA II. In this paper only B-spline surfaces were used, but NURBS and especially T-splines could be used for improvements and further reduction in the number of optimization variables.

Acknowledgment

This work was partly supported by the Croatian Science Foundation [Grant Number IP-2014-09-6130].

References

[1] Ray T, Gokarn RP, Sha OP. A global optimization model for ship design. Comput Ind 1995;26(2):175–92.
[2] Tahara Y, Peri D, Campana EF, Stern F. Computational fluid dynamics-based multiobjective optimization of a surface combatant using a global optimization method. J Mar Sci Technol 2008;13(2):95–116.
[3] Kim H, Yang C. A new surface modification approach for CFD-based hull form optimization. J Hydrodyn 2010;22(5 SUPPL. 1):503–8.
[4] Tahara Y, Peri D, Campana EF, Stern F. Single- and multiobjective design optimization of a fast multihull ship: numerical and experimental results. J Mar Sci Technol 2011;16(4):412–33.
[5] Jeong S, Kim H. Development of an efficient hull form design exploration framework. Math Probl Eng 2013;2013:1–12.
[6] Cui H, Turan O. Application of a new multi-agent hybrid co-evolution based particle swarm optimisation methodology in ship design. Comput Des 2010;42(11):1013–27.
[7] Cui H, Turan O, Sayer P. Learning-based ship design optimization approach. Comput Des 2012;44(3):186–95.
[8] Sarioz E. An optimization approach for fairing of ship hull forms. Ocean Eng 2006;33(16):2105–18.
[9] Pérez F, Clemente JA. Constrained design of simple ship hulls with -spline surfaces. Comput Des 2011;43(12):1829–40.
[10] Koelman HJ, Veelo BN. A technical note on the geometric representation of a ship hull form. Comput Des 2013;45(11):1378–81.
[11] Campana EF, Peri D, Tahara Y, Stern F. Shape optimization in ship hydrodynamics using computational fluid dynamics. Comput Methods Appl Mech Engrg 2006;196(1–3):634–51.
[12] Zhang Z, Liu H, Zhu S, Zhao F. Application of CFD in ship engineering design practice and ship hydrodynamics. J Hydrodyn 2006;18(3 SUPPL.):315–22.
[13] Hino T, Carrica P, Broglia R, Bull P, Kim SE, Li DQ, Wan D, Rhee SH, Saisto I, Viola IM. Specialist committee on CFD in marine hydrodynamics. In: 27th international towing tank conference, Vol. 2014, no. March 2012, p. 53.
[14] Sobey AJ, Blake JIR, Shenoi RA. Optimisation of composite boat hulls using first principles and design rules. Ocean Eng 2013;65:62–70.
[15] Sekulski Z. Multi-objective topology and size optimization of high-speed vehicle-passenger catamaran structure by genetic algorithm. Mar Struct 2010;23(4):405–33.
[16] Sun L, Wang D. A new rational-based optimal design strategy of ship structure based on multi-level analysis and super-element modeling method. J Mar Sci Appl 2011;10(3):272–80.
[17] Vučna D, Lozina Ž, Vlak F. NPV-based decision support in multi-objective design using evolutionary algorithms. Eng Appl Artif Intell 2010;23(1):48–60.
[18] Hart CG, Vlahopoulos N. An integrated multidisciplinary particle swarm optimization approach to conceptual ship design. Struct Multidiscip Optim 2009;41:481–94.
[19] Kim H, Yang C, Rainald L. A practical hydrodynamic optimization tool for the design of a monohull ship. In: ISOPE Conf., Vol. 8, 2008, p. 98–107.
[20] Peri D, Pinto A, Campana EF. Multi-objective optimisation of expensive objective functions with variable fidelity models. Large-Scale Nonlinear Optim 2006.
[21] Zhang P, Zhu D, Leng W. Parametric approach to design of hull forms. J Hydrodyn Ser B 2008;20(6):804–10.
[22] Abt C, Bade SD, Birk L, Harries S. Parametric hull form design — a step towards one week ship design. In: Proceedings of the eighth international symposium on practical design of ships and other floating structures, 2001, p. 67–74.
[23] Harries S, Abt C. Parametric curve design applying fairness criteria. In: International workshop on creating fair and shape-preserving curves and surfaces, 1998.
[24] ANSYS Inc., ANSYS (computer program). Ansys Inc., 2016.
[25] ITTC, ITTC – Recommended Procedures and Guidelines CFD, Resistance and Flow Benchmark Database for CFD Validation for Resistance and Propulsion, 1999.
[26] ITTC, ITTC – Recommended Procedures and Guidelines, Practical Guidelines for Ship CFD Application, 2011.
[27] Ahmed YM. Numerical simulation for the free surface flow around a complex ship hull form at different Froude numbers. Alex Eng J 2011;50(3):229–35.
[28] Olivieri A, Pistani F, Avanzini A, Stern F, Penna R. Towing Tank Experiments of Resistance, Sinkage and Trim, Boundary Layer, Wake, and Free Surface Flow Around a Naval Combatant Insean 2340 Model, Iowa, 2001.
[29] Tucker P, Pan Z. A Cartesian cut cell method for incompressible viscous flow. Appl Math Model 2000;24(8–9):591–606.
[30] Papanikolaou A. Holistic ship design optimization. Comput Des 2010;42(11):1028–44.
[31] Huetz L, Guillerm PE. Database building and statistical methods to predict sailing yacht hydrodynamics. Ocean Eng 2014;90:21–33.
[32] Sederberg MT, Sederberg TW. T-splines: a technology for marine design with minimal control points. In: Chesapeake Powerboat Symposium, 2010.
[33] Kostas KV, Ginnis AI, Politis CG, Kaklis PD. Ship-hull shape optimization with a T-spline based BEM–isogeometric solver. Comput Methods Appl Mech Engrg 2015;284:611–22.
[34] Ćurković M. Parameterization of 3D objects for numerical analysis and optimization of shape and topology. University of Split; 2014.
[35] Ćurković M, Vučina D. 3D shape acquisition and integral compact representation using optical scanning and enhanced shape parameterization. Adv Eng Informatics 2014;28(2):111–26.
[36] Várady T, Martin RR, Cox J. Reverse engineering of geometric models—an introduction. Comput Des 1997;29(4):255–68.
[37] Vučina D, Pehnec I. Enhanced reverse engineering using genetic-algorithms-based experimental parallel workflow for optimum design. Lecture notes in computer science, LNCS, Part 2 [(including subseries Lecture notes in artificial intelligence and lecture notes in bioinformatics)], vol. 6625. 2011. p. 172–83.
[38] Vućina D, Milas Z, Pehnec I. Reverse shape synthesis of the hydropump volute using stereo-photogrammetry, parameterization, and geometric modeling. J Comput Inf Sci Eng 2012;12(2):021001.
[39] Milas Z, Vučina D, Marinić-Kragić I. Multi-regime shape optimization of fan vanes for energy conversion efficiency using CFD, 3D optical scanning and parameterization. Eng Appl Comput Fluid Mech 2014;8(3):407–21.
[40] Becker G, Schäfer M, Jameson A. An advanced NURBS fitting procedure for post-processing of grid-based shape optimizations. In: 49th AIAA aerosp. sci. meet. incl. new horizons forum aerosp. expo., no. January, 2011.
[41] MathWorks, MATLAB (computer program). 2015.
[42] Esteco s.p.a, modeFRONTIER (computer program). Esteco s.p.a, 2014.
[43] Poles S. MOGA-II An Improved Multi-Objective Genetic Algorithm, Trieste, 2003.
[44] Sobol IM, Asotsky D, Kreinin A, Kucherenko S. Construction and comparison of high-dimensional sobol ' generators. Wilmott Mag 2011;64–79.
[45] Zakerdoost H, Ghassemi H, Ghiasi M. Ship hull form optimization by evolutionary algorithm in order to diminish the drag. J Mar Sci Appl 2013;12(2):170–9.
[46] Sareni B, Krähenbühl L. Fitness Sharing and Niching Methods Revisited. IEEE Trans E Comput 1998;2(3):97–106.

Please cite this article in press as: Marinić-Kragić I, et al. Efficient shape parameterization method for multidisciplinary global optimization and application to integrated ship hull shape optimization workflow. Computer-Aided Design (2016), http://dx.doi.org/10.1016/j.cad.2016.08.001